Phase separation in manganite thin films

2008 J. Phys.: Condens. Matter 20 434232

(http://iopscience.iop.org/0953-8984/20/43/434232)

J. Phys.: Condens. Matter **20** (2008) 434232 (5pp) doi:10.1088/0953-8984/20/43/434232

Phase separation in manganite thin films

A Antonakos[1], D Lampakis[1], E Liarokapis[1], M Filippi[2], W Prellier[2], G H Aydogdu[3] and H-U Habermeier[3]

[1] Department of Physics, National Technical University, GR-15780 Athens, Greece
[2] Laboratoire CRISMAT, CNRS UMR 6508, ENSICAEN, 6 Boulevard Marechal Juin, F-14050 Caen Cedex, France
[3] Max-Planck-Institute for Solid State Research, Stuttgart, D-70569, Germany

E-mail: tantonak@central.ntua.gr

Received 7 July 2008
Published 9 October 2008
Online at stacks.iop.org/JPhysCM/20/434232

Abstract

Thin films of $R_{1-x}Ca_xMnO_3$ (R = La, Pr) manganites deposited on different substrates have been studied by micro-Raman spectroscopy. The macroscopic transport and magnetic properties of the films are affected by the structural changes and the strain effects, due to the different R and Ca ($0.4 \leqslant x \leqslant 0.6$) doping or epitaxial strains. Despite the similar average structure obtained by diffraction techniques, in the Raman spectra the metallic rhombohedral-like R–O(1) bending and Mn–O–Mn or octahedra tilting modes coexist with the broad Jahn–Teller (JT) stretching bands, characteristic of the insulating phase. The intensity of the broad JT bands is related to the amplitude of the cooperative or dynamic octahedron distortions and the charge-ordered phases. Based on a percolation picture, we attribute the spectral modifications to a mesoscopic phase separation.

1. Introduction

Phase separation (PS) seems to be a generic feature of doped strongly correlated systems such as rare-earth manganites with the general formula $R_{1-x}A_xMnO_3$ (R being a trivalent rare-earth ion and A a divalent alkaline-earth ion). The complex interplay between the spin, lattice, and charge degrees of freedom is responsible for the exotic magnetic and electronic phases that coexist [1, 2]. This coexistence is self-organized, very sensitive to internal (doping concentration, average atomic radius $\langle r_A \rangle$) and external perturbations (temperature, pressure, and magnetic field), and results in metallic phases being converted into insulating ones or vice versa, supporting the existence of metastable phases. This behavior has been observed in many theoretical and experimental results [1, 3, 4], especially close to the half-doping region ($x = 0.5$).

There are studies outlining the importance of long-range lattice strains for understanding the PS scenario [5, 6]. Lattice distortions may be related to oxygen displacements or to the Jahn–Teller (JT) effect perturbing the e_g electrons of the MnO_6 octahedra [7]. In addition, as a result of the replacement of the trivalent R ions by the divalent A ions, the octahedra are distorted and tilted cooperatively in order to optimize the R–O bonds [6]. According to these models epitaxial strains in thin films lead to changes of their physical properties [8]. Their study can help to understand the role of lattice distortions in PS phenomena.

In this paper we present results for $La_{0.5}Ca_{0.5}MnO_3$ (LCMO) and $Pr_{1-x}Ca_xMnO_3$ ($0.4 \leqslant x \leqslant 0.6$) (PCMO) thin films grown on different substrates that induce high in-plane compressive or tensile strains. It is a common opinion that LCMO($x = 0.5$) and PCMO compounds are always phase separated and the ferromagnetic metallic regions coexist with the antiferromagnetic and charge-ordered ones. The LCMO($x = 0.5$) bulk compound is a paramagnetic (PM) insulator and at low temperatures first undergoes a ferromagnetic (FM) and then a simultaneous AFM and charge ordering (CO) transition [9]. The charge-ordered (CO) phase of PCMO occurs in the region $0.3 \leqslant x \leqslant 0.75$ at a temperature in the range 220–260 K (T_{CO}), that depends on the amount of Ca doping [10, 11]. This ordering phenomenon is optimized for $x = 0.5$, where the carriers are exactly commensurate with the 1:1 ordering of the Mn^{3+}:Mn^{4+} ions. Within this CO phase, there is a magnetic transition to an AF insulating (AFI) phase at temperature $T_N < T_{CO}$. Raman spectroscopy is an excellent tool for providing information about the local structure of the different phases present in manganites [12]. It was found that the spectral modifications were correlated with the JT distortions; in highly doped compounds with weak JT distortions rhombohedral-like sharp bands appear, while in the spectra of compounds with strong JT distortion strong broad

JT bands appear. We have found evidence for the presence of insulating regions coexisting with FM metallic (FMM) ones, which most likely originate at an inhomogeneous strain field.

2. Experimental details

The LCMO($x = 0.5$) and PCMO films were developed by the pulsed laser deposition (PLD) technique. X-ray diffraction studies have shown that the films were of single phase and highly crystallized. It has been found that the PCMO films were (101) oriented on the $LaAlO_3$ (LAO) substrate and (010) oriented on the $SrTiO_3$ (STO) substrate. The difference was due to the lattice mismatch between film and substrate [13]. A more detailed analysis for the PCMO thin films is described elsewhere [14, 15]. For the LCMO($x = 0.5$) films on the (100) STO and the (001) $SrLaGaO_4$ (SLGO) substrates, the (020) planes of the films were identified to be parallel to the substrate (*b*-axis oriented). However, films on (111) STO were oriented along the (022) direction. A more analytical discussion about the preparation and characterization methods (XRD, magnetization, resistivity) is presented elsewhere [16].

The Raman spectra were obtained using a T64000 Jobin-Yvon triple spectrometer, equipped with liquid nitrogen cooled charge coupled device (CCD) and a microscope. The 514.5 nm line of an Ar^+ laser was used for excitation at low power, which was kept fixed during the measurements at the level of ∼0.2 mW on the surface of the film. The low temperature measurements were carried out in an Oxford cryostat. A backscattering geometry was used, with the sample placed under the microscope with 100× magnification. A Merrill-Bassett type diamond anvil cell (DAC) was used for the high-pressure measurements, which allowed the Raman studies to be carried out in a backscattering geometry. The pressure-transmitting medium was a mixture of methanol and ethanol. By including several small silicon crystals inside and outside the DAC and the cryostat, the effect of pressure could be discriminated from that induced by the low temperature or any misalignment of the spectrometer during the measurement. Besides, the pressure was calibrated and the hydrostatic environment was continuously inspected.

3. Results

The orthorhombic $RMnO_3$ is structurally distorted with respect to the cubic perovskite in two ways: the MnO_6 octahedra present a strong JT cooperative distortion due to Mn^{3+} ions, and the octahedra are tilted in order to optimize the R–O bond lengths [12]. The *Pnma* structure of the films (as detected by the XRD studies) gives $7A_g + 5B_{1g} + 7B_{2g} + 5B_{3g}$ Raman active zone-center optical phonons, which are activated exclusively due to the deviations from the ideal perovskite structure.

Figure 1 shows typical Raman spectra of the thin films at room temperature (RT). In all spectra the low frequency bands (ω_1) are generally attributed to R–O modes, which correspond to mixed R and O1 vibrations around the xz plane (A_g and B_{2g} symmetry modes) or the y axes (B_{1g} and B_{3g} modes) [17]. Modes related to the tilting of the octahedra are expected at

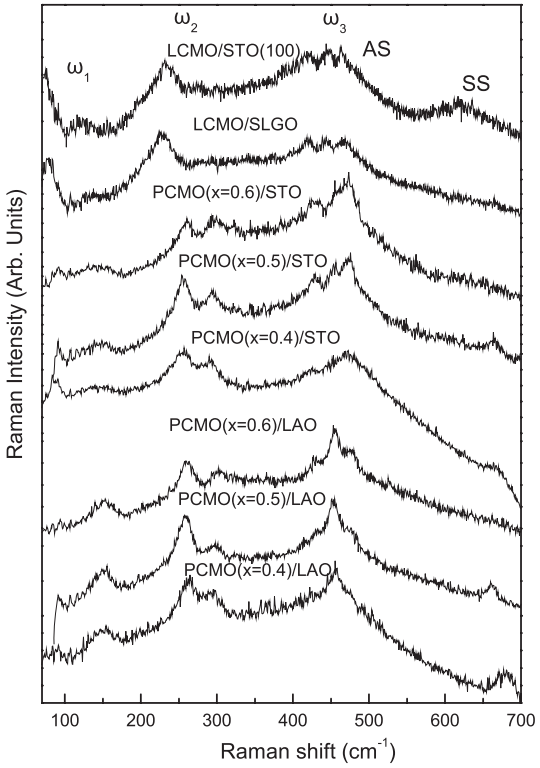

Figure 1. Typical Raman spectra at RT of all manganite thin films in parallel backscattering polarization geometry using the 514.5 nm excitation wavelength.

200–300 cm^{-1} (ω_2), the bending modes are associated with the 400–500 cm^{-1} (ω_3) region, while the JT stretching modes are connected with bands at ∼480 cm^{-1} (antisymmetric, AS) and ∼610 cm^{-1} (symmetric, SS) for both $RMnO_3$ as well as in doped compounds [12]. Figure 2 presents typical Raman spectra of the thin films at 80 K.

The R–O modes are mainly affected by the ion size strain while the epitaxial strain seems to have negligible effect on their frequencies (figure 1). The phonons gain intensity with decreasing temperature, while their energy appears independent of temperature (figures 1 and 2).

In the ω_2 region at RT the $A_g(2)$ mode appears very strong, while its neighboring peak at higher frequencies is assigned to the $A_g(4)$ phonon and is better observed in PCMO thin films (figure 1). In addition, in these films the ω_2 bands are observed at higher frequencies as a result of the R substitution [12]. Raman scattering in the PCMO [18–21] and LCMO($x = 0.5$) [22] compounds reveals that the strong coupling between spin and charges induces variations in the mode frequencies and widths of the tilting $A_g(2)$ and $A_g(4)$ phonons.

In the ω_3 region the spectra consist of at least three bands (figure 1). In the PCMO thin films with increasing x from 0.4 to 0.6 the broad (ω_3) region loses weight at the high frequency side, while the 425 cm^{-1} band is better distinguished at $x = 0.6$. In addition, the JT SS mode disappears for $x = 0.6$. In the LCMO thin films the three sharp ω_3 bands are observed at lower frequencies than in PCMO and are better distinguished. In the LCMO($x = 0.5$)/STO(100) thin film strong JT SS broad

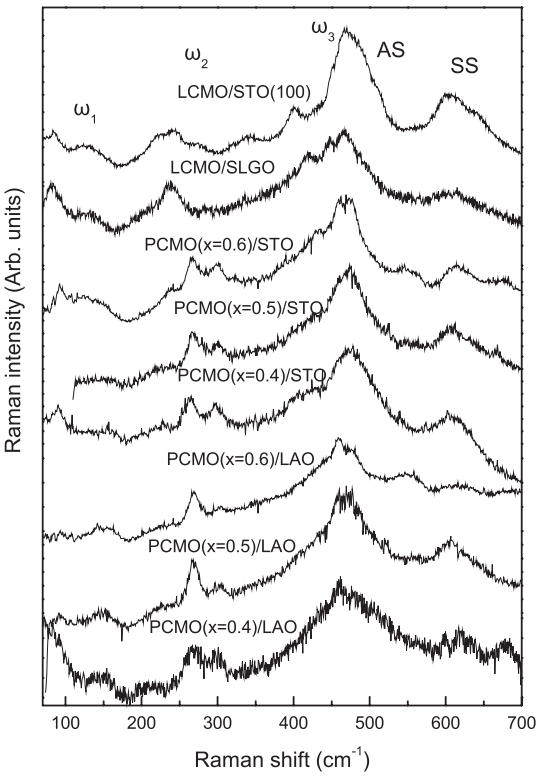

Figure 2. Typical Raman spectra at 80 K of all manganite thin films in parallel backscattering polarization geometry using the 514.5 nm laser line.

bands appear, while in LCMO($x = 0.5$)/SLGO this mode is not observed at RT.

With decreasing temperature below T_{CO} the main characteristics of the Raman spectra in all thin films are the very strong stretching modes in the CO phase (figure 2). The recovery of the stretching phonon peaks is understood as being caused by the orbital ordering and the concomitant cooperative JT distortion [12].

4. Discussion

The doping and epitaxial strain is expected to affect the properties of the lattice and carriers. Martin-Carron *et al* [12] proposed that the type of spectra and the intensity of the JT modes can be used to estimate the cooperative or dynamical JT distortion. In addition, the frequencies of the modes can be used to identify the structural changes. It should be noted that the bending modes involve modifications of the Mn–O–Mn angle and stretching of the R–O(1) bond length [12]. The R–O bonds are also related to the R modes. The force constants of the stretching Mn–O modes depend on the interatomic distances and the observed modifications can be ascribed to a symmetrization of the MnO_6 octahedra and a reduction of the JT distortion [23]. As mentioned above, the octahedra are tilted in order to optimize the R–O bond lengths and the Mn–O–Mn angle.

The frequency of the $A_g(2)$ mode in the $RMnO_3$ compounds has been correlated with the dependence of the tilting angle on the Ca and R doping [12]. Similar to the curve fitted for the LCMO compound by Martin-Carron *et al* [12] for Ca doping dependence (due to the similarity of the Pr and La ionic radii), the $A_g(2)$ mode frequency at $x = 0.5$ of the PCMO thin films appears slightly smaller than its values at $x = 0.4$ and $x = 0.6$. The effect of R substitution on the tilting angle appears to be much stronger, since the $A_g(2)$ mode appears $\sim$20 cm^{-1} lower on the LCMO thin films. For thin films with the same composition the $A_g(2)$ mode frequency changes $\sim$3 cm^{-1} depending on the substrate, due to the different type and amplitude of epitaxial strain [13, 16]. Therefore, several perturbations (R and Ca doping, magnetic field [21], pressure [24, 20] and epitaxial strains) affect the tilting of the octahedra, as can be detected by the $A_g(2)$ mode.

The ω_3 region is also mainly affected by the R substitution. The bending mode frequencies are correlated with the R–O(1) bond length, as already mentioned. Therefore, the three sharp bending peaks in the LCMO($x = 0.5$) thin films appear at lower frequencies than in the Pr substitution for La PCMO films. The JT AS mode is expected at $\sim$480 cm^{-1} [12]. This can explain why the bending modes are better distinguished in LCMO than in the PCMO thin films where the JT AS mode is partially obscured by the 476 cm^{-1} bending mode, in agreement with [25]. Therefore, one would expect the ω_3 region to lose weight with doping due to the decreased intensity of the JT AS mode. In addition, with increasing doping the other JT (SS) mode disappears. So, we can conclude that the JT dynamical distortion is reduced as doping increases. In the LCMO($x = 0.5$) thin films, there is an epitaxial strain-induced effect on the dynamical JT distortion. LCMO($x = 0.5$)/STO(100) films have larger JT distortions than LCMO($x = 0.5$)/SLGO, as suggested by the decreased broad stretching modes in the latter. The reduction of the JT distortion may cause enhancement of the double exchange mechanism and in turn make the sample more conductive, as confirmed by the resistivity measurements [16]. The reduction of the JT distortion and the pressure effects on the phase separation of PCMO($x = 0.4$)/LAO thin films is the main reason of the decrease in resistivity under pressure [24].

In a previous work it has been shown that the JT modes couple with the CO phase and gain considerable intensity across T_{CO} [20]. By comparing the JT intensity on the low temperature spectra (figure 2) we can estimate the charge localization on the thin films. On the LCMO($x = 0.5$) thin films, the substrate has a big effect on the CO phase. For the LCMO($x = 0.5$)/SLGO film, both stretching modes are considerably decreased. The tilting and bending modes are attributed to the metallic rhombohedral-like phase peaks [12]. The reduction of the JT distortion weakens the electron–phonon coupling and induces charge delocalization [26]. The destruction of the CO phase must be the main reason for the observed insulator to metal (IM) transition under pressure on bulk PCMO [27]. In addition, the phase separation phenomenon is regarded as an important factor for the large resistivity change that accompanies the first order IM transition [28]. In a recent study, it has been suggested by Raman spectroscopy that due to a strain-induced effect on the phase separation of the LCMO/STO(100) thin films, the AF

phase dominates and the FM phase is destroyed, contrary to the bulk where both phases coexist down to 5 K [22]. This gives strong evidence that phase separation plays an important part in the IM transition in the bulk. The increased intensity and the reduced width of the 'metallic' peaks are attributed to FMM clusters formed in the insulating phase, which is characterized by the JT broad bands [12].

Concerning the PCMO samples, it was found that the critical magnetic field to destroy CO is strongly reduced when the compound is made in the form of a thin film [8]. In addition, it was found that in the PCMO($x = 0.5$)/STO films a magnetic field of 6 T is required to induce an IM transition [8], while a magnetic field of 7 T is not strong enough to destroy the CO phase in PCMO($x = 0.5$)/LAO and the behavior of the compound is semiconducting [15]. The JT SS mode appears stronger at $x = 0.5$ with respect to the other two Ca doping levels in both substrates (figure 2). This is additional strong evidence that this mode couples with the CO phase, which is optimized and robust at this point [27]. The JT AS mode is also suppressed when we go away from the CO phase optimization point ($x = 0.5$). The effect of pressure on the Raman spectra of PCMO($x = 0.4$)/LAO thin films has been studied in a recent work and the macroscopic resistivity behavior was correlated with the similar trend of the relative intensities of the broad JT modes of the insulating phase to the sharp metallic-like phase peaks [24]. The results are explained by a pressure-induced phase separation scenario where FMM domains coexist with the insulating states, providing a good description of the semiconducting behavior of the thin films. A similar unusual insulating FM state under a magnetic field has been detected for PCMO($x = 0.5$)/LAO thin films [15].

Correlation of the microscopic observations of the Raman spectra with the macroscopic transport and magnetic properties can be better described by the phase separation scenario on the percolation picture. The manipulation of the phase separation by epitaxial strains, doping and the hydrostatic pressure is summarized in figure 3. The FMM clusters (white) appear in the insulating matrix (black) at RT for all samples. The total concentration of the metallic phase is affected by the former perturbations and it is different for each film. In PCMO thin films with decreasing temperature, the CO phase is considerably increased and the FM droplets shrink, leading to the insulating behavior of the films at low temperature. Under pressure, FMM cluster droplets are first formed close to nucleation centers and then grow leading to a more conductive behavior, but the percolation limit is not reached. The strain effects on the LCMO ($x = 0.5$)/STO(100) thin film destroy the FM phase and the CO phase is more robust than the bulk compound, leading to the AFM/CO insulating phase at low temperature. On the contrary, the FMM clusters grow and start to coalesce until the percolation limit is reached on the LCMO ($x = 0.5$)/SLGO thin film, and the system behaves like a metal.

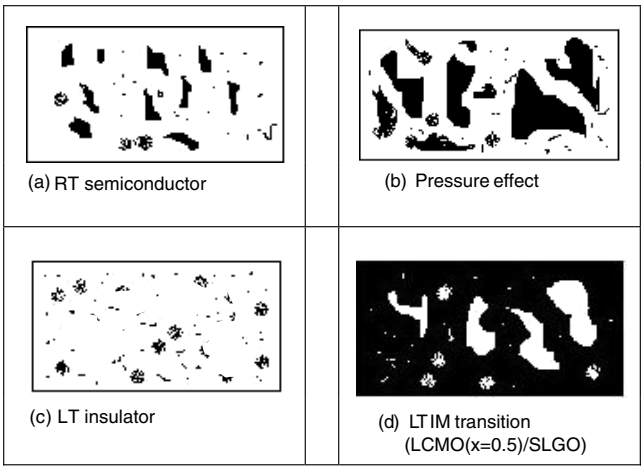

Figure 3. Schematic representations of the phase separation scenario in the percolation picture. (a) For all thin films at ambient conditions (RT, $p = 0$) small FMM clusters (black regions) are formed on the insulating phase (white matrix). (b) At high pressures ($p = 4.5$ GPa) bigger FMM clusters are formed and the compound is more conductive. However, the system does not cross the percolation limit. (c) The AFM/CO insulating phase is increased and the FMM clusters shrink for all the PCMO thin films and the LCMO($x = 0.5$)/STO(100) thin film at low temperature. (d) The IM transition for the LCMO($x = 0.5$)/SLGO thin film. The percolation limit is reached and there are insulating clusters on the FMM matrix.

5. Conclusions

Thin films of $R_{1-x}Ca_xMnO_3$ (R = La and Pr) grown on LAO, STO and SLGO substrates have been investigated by Raman spectroscopy. Based on spectral analysis and the coexistence of modes characteristic of the metallic phase with others attributed to the Jahn–Teller distortions that identify an insulating charge-ordered behavior, we conclude that the compound has undergone phase separation into metallic and insulating domains. The overall physical properties with doping and under varying external conditions could be explained assuming a percolative motion of the carriers among the metallic nanodomains.

Acknowledgments

Work supported through the project E.C. STREP no 517039 'COMEPHS'. The authors want to thank P Auban-Senzier and C Pasquier for the resistivity experiments.

References

[1] Dagotto E, Hotta T and Moreo A 2001 *Phys. Rep.* **344** 1
[2] Salamon M B and Jaime M 2001 *Rev. Mod. Phys.* **73** 583
[3] Nagaev E L 1996 *Phys. Usp.* **39** 781
[4] Khomskii D I 2000 *Physica* B **280** 325
[5] Ahn K H, Lookman T and Bishop A R 2004 *Nature* **428** 401
[6] Burgy J, Moreo A and Dagotto E 2004 *Phys. Rev. Lett.* **92** 97202
[7] Millis A J, Littlewood P B and Shraiman B I 1995 *Phys. Rev. Lett.* **74** 5144
[8] Prellier W, Lecoeur Ph and Mercey B 2001 *J. Phys.: Condens. Matter* **13** R915
[9] Iliev M N and Abrashev M V 2001 *J. Raman Spectrosc.* **32** 805
[10] Martin C, Maignan A, Hervieu M and Raveau B 1999 *Phys. Rev.* B **60** 12191
[11] Tokura Y and Tomioka Y 1999 *J. Magn. Magn. Mater.* **200** 1
[12] Martin-Carron L, de Andres A, Martinez-Lope M J, Casais M T and Alonso J A 2002 *Phys. Rev.* B **66** 174303

[13] Prellier W, Simon Ch, Haghiri-Gosnet A M, Mercey B and Raveau B 2000 *Phys. Rev.* B **62** R16337
[14] Prellier W, Haghiri-Gosnet A M, Mercey B, Lecoeur Ph, Hervieu M, Simon Ch and Raveau B 2000 *Appl. Phys. Lett.* **77** 1023
[15] Haghiri-Gosnet A M, Hervieu M, Simon Ch, Mercey B and Raveau B 2000 *J. Appl. Phys.* **88** 3545
[16] Aydogdu G H, Kuru Y and Habermeier H U 2007 *Mater. Sci. Eng.* B **144** 123
[17] Iliev M N, Abrashev M V, Lee H-G, Popov V N, Sun Y Y, Thomsen C, Meng R L and Chu C W 1998 *Phys. Rev.* B **57** 2872
[18] Dediu V, Ferdeghini C, Matacotta F C, Nozar P and Ruani G 2000 *Phys. Rev. Lett.* **84** 4489
[19] Gupta R, Venketeswara Pai G, Sood A K, Ramakrishnan T V and Rao C N R 2002 *Europhys. Lett.* **58** 778
[20] Tatsi A, Papadopoulou E l, Lampakis D, Liarokapis E, Prellier W and Mercey B 2003 *Phys. Rev.* B **68** 024432
[21] Antonakos A, Lampakis D, Palles D, Liarokapis E, Prellier W and Mercey B 2007 *J. Magn. Magn. Mater.* **310** 2164
[22] Antonakos A, Liarokapis E, Aydogdu G H and Habermeier H-U 2007 *Mater. Sci. Eng.* B **144** 83
[23] Martyn-Carron L, Sanchez-Bentez J and de Andres A 2003 *J. Solid State Chem.* **171** 313
[24] Antonakos A, Lampakis D, Liarokapis E, Filippi M, Prellier W, Auban-Senzier P and Pasquier C 2008 Pressure effects on the phase separation of $Pr_{0.6}Ca_{0.4}MnO_3$ thin films *J. Phys.: Condens. Matter* submitted
[25] Iliev M N, Abrashev M V, Laverdiere J, Jandl S, Gospodinov M M, Wang Y-Q and Sun Y-Y 2006 *Phys. Rev.* B **73** 064302
[26] Postorino P, Dore P, Congeduti A, Sacchetti A, Ulivi L, Gorelli F A, Kumar A and Sarma D D 2003 *Phys. Rev. Lett.* **91** 175503
[27] Cui C and Tyson T A 2004 *Phys. Rev.* B **70** 094409
[28] Ghivelder L, Freitas R S, das Virgens M G, Continentino M A, Martinho H, Granja L, Quintero M, Leyva G, Levy P and Parisi F 2004 *Phys. Rev.* B **69** 214414